Magnetic susceptibility and spin-glass behavior in the pseudo-one-dimensional mixed system $[(CH_3)_3NH]Co_{1-x}Ni_xCl_3\cdot 2H_2O$ and the analogous Co-Mn and Ni-Mn systems

Gerald V. Rubenacker, David P. Raffaelle, and John E. Drumheller
Department of Physics, Montana State University, Bozeman, Montana 59717

Kenneth Emerson
Department of Chemistry, Montana State University, Bozeman, Montana 59717
(Received 27 January 1986; revised manuscript received 24 July 1987)

The magnetic behavior of the pseudo-one-dimensional mixed systems $[(CH_3)_3NH]A_{(1-x)}B_xCl_3\cdot 2H_2O$, where A and B are Co, Ni, and Mn, have been investigated as a function of x. The mixture with Co and Ni has been found to exhibit spin-glass behavior below a characteristic temperature T_g as evidenced by the onset of time-dependent thermoremanent magnetization. The phase diagram of temperature versus x shows a very broad and deep spin-glass region with unusually thin antiferromagnetic phase regions above it. Evidence for a tetracritical point near $x=0.58$ is indicated. Thermoremanent magnetization versus time below T_g has been fit to a stretched exponential function plus a constant offset. Since the mixtures with Mn with Co and Mn with Ni show no spin-glass behavior, these systems show that the critical dimensionality for spin-glass behavior must be greater than one.

INTRODUCTION

Many papers have been published on the pseudo-one-dimensional compounds $[(CH_3)_3NH]MCl_3\cdot 2H_2O$ in which M is Co, Ni, Mn, Cu, or Fe, hereafter abbreviated as $MTAC$, in which M again denotes the metal or metals involved. Of specific interest in this paper are the mixed magnetic systems Co-NiTAC, Mn-CoTAC, and Mn-TiTAC with special emphasis on Co-NiTAC. Prior work by other authors on the pure Co, Ni, and Mn compounds will be briefly reviewed below. Co-NiTAC is particularly interesting because of the history dependence of the magnetization below a temperature which we will call T_g. The thermoremanent magnetization (TRM) seen in this site disordered system is similar to that found in classical metallic spin glasses and will be discussed in terms of a spin-glass state.[1-5] Indeed the TRM in Co-NiTAC can be fit to a stretched exponential decay typical of certain classes of spin glasses. Also interesting is the fact that the Mn-CoTAC and the Mn-NiTAC compounds do not show TRM or other signs of spin-glass behavior.

The structure of CoTAC, the pure cobalt analog, was determined by Lossee *et al.*[6] and consists of linear chains of Co atoms coupled via two Co—Cl—Co bonds. This is the strongest exchange path with $J_b/k=15.4$ K, were b denotes the crystallographic b direction and also the chain direction. This interaction is ferromagnetic, as is the next strongest coupling in the c-axis direction. Since this exchange is through bonds with the H_2O ligands, the coupling is much smaller; $J_c/k=0.1$ K. There is virtually no direct exchange path in the third direction and $J_a/k=-0.01$ K is smaller still. This exchange is negative, therefore, the overall three-dimensional ordering is antiferromagnetic with a critical temperature, $T_c=4.2$ K. The antiferromagnetic or easy axis is along the c direction. The a axis shows weak ferromagnetic behavior indicating that the spins are canted away from c in the a direction. The b-axis susceptibility is very small indicating that the spins are confined to the ac plane. NMR studies by Spense and Botterman[7] originally predicted the canting angle to be about 10° from the c direction. They also show a transition at about 60 Oe from an antiferromagnetic to paramagnetic state along the c axis, making this compound a metamagnet. Further ac susceptibility measurements by Groenendijk and van Duyneveldt[8,9] confirmed the metamagnetic behavior but predict a zero-field canting angle of 22°.

The structure of NiTAC was determined by O'Brien *et al.*[10] and is nearly identical to CoTAC. The reported magnetic parameters are also similar with $T_c=3.7$ K, $J_b/k=14$ K, $J_c/k=0.07$ K, and $J_a/k=-0.006$ K as determined by Hoogerbeets *et al.*[11] The spins are again confined to the ac plane with a canting angle of 21° from the c direction. EPR studies by Hoogerbeets *et al.*[12] confirm the c axis to be the easy axis and b to be the hard axis.

The structure of MnTAC was determined by Caputo *et al.*[13] and by Depmeier *et al.*[14] MnTAC is also isomorphic to its cobalt and nickel analogs, but in contrast, has antiferromagnetic coupling along the chains with a Néel temperature of $T_n=4.1$ K as determined by Simizu *et al.*[15] The phase diagram for this compound near the bicritical point has also been determined by Megy *et al.*[16]

Because of the structural similarity of these three compounds and their well-documented magnetic behavior, we chose to begin studying these three mixed systems. Since MnTAC is an antiferromagnetic and CoTAC and NiTAC are ferromagnets, we originally expected the mixed Mn-Ni and Mn-Co systems to be the most likely candidates for spin-glass behavior. However, it is the Co-NiTAC system, and not the manganese systems, that

appears to show spin-glass behavior.

We know of three previous papers on these mixed systems. Schouten *et al.*[17] studied the phase diagram of CoCu*TAC* using heat-capacity measurements. The data fit best to a bond impurity model in which the Cu-Cu interactions are small while the Co-Cu and Co-Co interactions are nearly identical. Matsubara *et al.*[18] and Phaff *et al.*[19] did spin resonance work on MnCo*TAC* compounds indicating a decreased coupling between Mn and Co resulting in a limiting of the spin diffusion rate.

CRYSTAL PREPARATION

Crystalline samples of CoNi*TAC* were all prepared by mixing aqueous solutions of $CoCl_2$, $NiCl_2$, and $[(CH_3)_3NH]Cl$ in appropriate amounts and letting the solutions evaporate slowly at room temperature. These compounds are exceedingly soluble so the solutions used for crystallization were very concentrated. All samples were removed from the mother liquor soon after crystallization began, washed with 95% ethanol, and allowed to air dry. MnCo*TAC* and MnNi*TAC* samples were prepared similarly.

The crystals formed do not contain the same metal percentages as the solutions from which they were prepared. A graph of nickel as a percent of the total metal in the preparative solution and the mole fraction of nickel in the crystals for CoNi*TAC* is presented in Fig. 1. The nickel and cobalt fractions in the crystals were determined by atomic adsorption spectroscopy. The MnCo*TAC* and MnNi*TAC* systems have a similar solution versus crystal composition behavior.[20]

EXPERIMENT

Magnetization data were taken using an EG&G PAR model 155 vibration sample magnetometer equipped with a Janis liquid-helium cryostat. By pumping on the sample space, temperatures down to about 2 K were reached. Magnetization data were obtained on powder samples of about 80 mg and on small crystals weighing about 0.3 mg.

$1/\chi$ versus temperature for powder samples of all three mixed systems were plotted to determine the Curie temperature T_C for long-range ordering. These temperatures are summarized in Table I along with the corresponding nickel content as a percentage of total metal.

The "spin-glass" transition temperatures T_g were determined by observing the TRM at various temperatures in the powder samples. A field of 1000 Oe was applied at a temperature above T_C. The temperature was then lowered to typically 2 K and the field was switched to zero Oe. The remanant magnetization was then measured as a function of time at various temperatures below T_C. Figure 2 shows the TRM data for the 65%-nickel sample plotted as a function of temperature for various waiting times and is representative of all of the CoNi*TAC* samples. As the temperature is increased the remanant magnetization falls to zero indication the high-temperature boundary of the spin-glass region. No TRM was found for the pure nickel or pure cobalt compounds, nor for the MnCo*TAC* or the MnNi*TAC* mixtures at the lowest temperature available from our equipment (2 K).

The TRM versus time was also examined in the CoNi*TAC* systems at 34%, 58%, and 72% nickel for temperatures between 2.4 and 3.2 K for the powder samples in order to determine the functional form of the decay of the magnetization. A field of 50 Oe was applied above T_C, temperature was lowered at a rate of about 0.05 K/sec, the system was allowed to stabilize at the desired temperature for about 30 sec, and the field was switched to 0 ± 0.05 Oe. TRM versus time for 34% nickel for various temperatures is shown in Fig. 3 as an example. Because of a mechanical delay of 5 sec in lowering the field to zero and a 1-sec time constant in the magnetometer, data for times shorter than 10 sec could not be taken with confidence. A model to fit these TRM measurements will be considered in the next section.

The powder data have been emphasized in this work

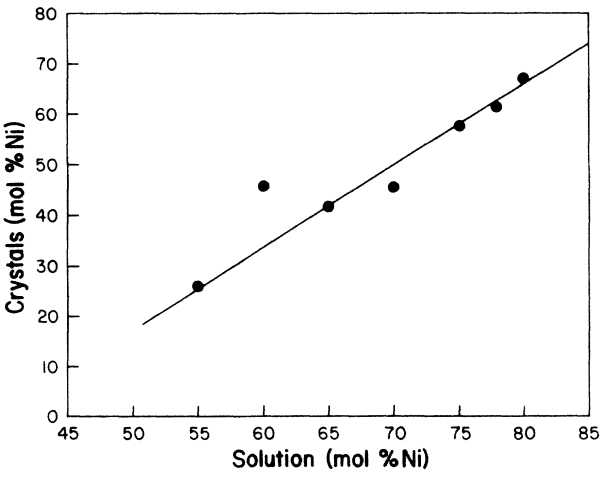

FIG. 1. Percent nickel in the solutions used to prepare the mixed CoNi*TAC* samples vs percent nickel in the resultant crystals.

TABLE I. Antiferromagnetic transition temperatures T_C and spin-glass transition temperatures T_g for various percentages of nickel in $[(CH_3)_3NH]Co_{(1-x)}Ni_xCl_3\cdot 2H_2O$.

% Ni	T_C	T_g
0	5.135[a]	
21	4.14	3.5
34	4.12	3.6
42	4.14	3.6
50	4.14	3.55
53	4.18	3.75
56	4.10	3.75
58	4.02	3.9
60	4.08	3.75
65	4.18	3.55
68	4.10	3.4
72	4.10	3.4
100	3.6[b]	

[a]Reference 6.
[b]Reference 10.

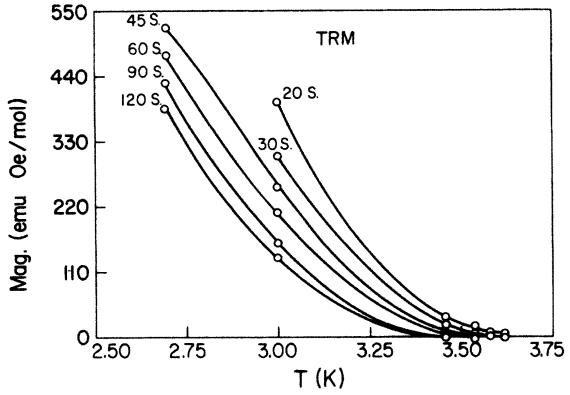

FIG. 2. Thermoremanent magnetization (1-kOe initial field) vs temperature for various waiting times in the 65%-nickel sample. T_g is denoted as the point at which no TRM is seen.

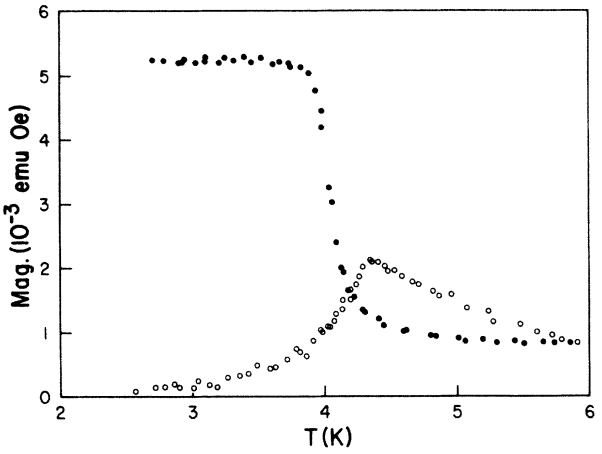

FIG. 4. Magnetization vs temperature at 50 Oe for a single crystal of CoNiTAC containing 37% nickel. Open circles are for the c axis (antiferromagnetic) and solid circles are for the a axis (ferromagnetic).

because the larger sample sizes permitted more sensitive measurements. However, to emphasize anisotropies and to determine easy axes, some single-crystal samples have been measured in the CoNiTAC systems. Figure 4 shows the results from 3 to 5 K for a 37%-Ni sample along both the a and c axes in a field of 50 Oe. Measurements along the b axis for these small crystals are below the resolution of our apparatus. The c (easy) axis shows the overall three-dimensional, antiferromagnetic ordering, while the a axis shows a ferromagnetic ordering due to the spin canting in this direction. Figure 5 is a plot of magnetization versus applied field along the c axis for this same sample at 3 K and shows an antiferromagnetic to spin-flop transition at about 200 Oe. Thermoremanent magnetization was also examined on the single crystals and was found to be localized along the a or ferromagnetically canted direction with no TRM in the c direction. Because of small signal sizes no quantitative fitting of the single-crystal TRM's was attempted.

In order to verify the existence of the spin-glass phase which we observe in the dc magnetization data, ac susceptibility data in a zero field has been obtained. Using an ac superconducting quantum interference device (SQUID) susceptometer, a steep rise is seen in the susceptibility followed by a sharp decrease as temperature is lowered to below T_g. This cusp is observed only along the a or ferromagnetic axis in CoNiTAC.[21]

DISCUSSION

The phase diagram for this system as constructed from the nickel percentages and transition temperatures for the powder samples in Table I is shown in Fig. 6. At high temperatures the sample exists in a paramagnetic phase which, as temperature is lowered, enter a canted antiferromagnetic phase and then the spin-glass phase. The line on the diagram represents the highest temperatures at which thermoremanent magnetization is observed. As illustrated in Fig. 3, freezing of the spins occurs gradually as temperature is lowered.

We have considered the possibility that the time-

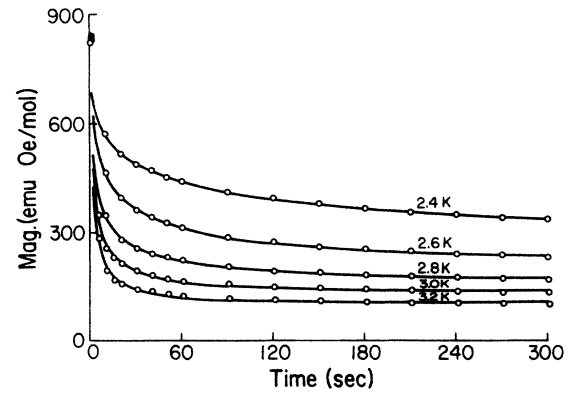

FIG. 3. Thermoremanent magnetization vs time (50-Oe initial field) for the 34% sample at 2.4, 2.6, 2.8, 3.0, and 3.2 K. The solid lines are fit to a stretched exponential with a constant offset.

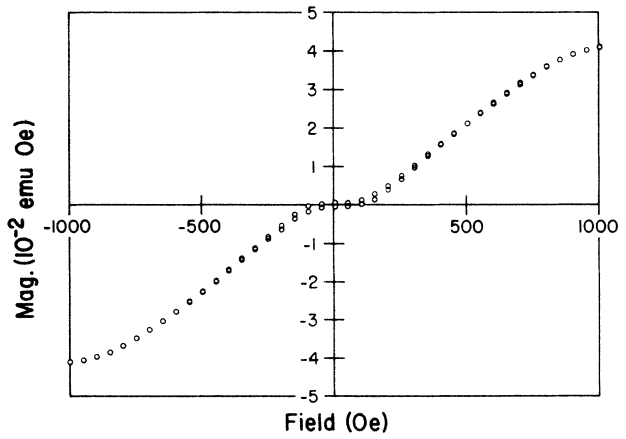

FIG. 5. Magnetization vs applied field for a single crystal of CoNiTAC containing 37% nickel and oriented along the c or antiferromagnetic axis.

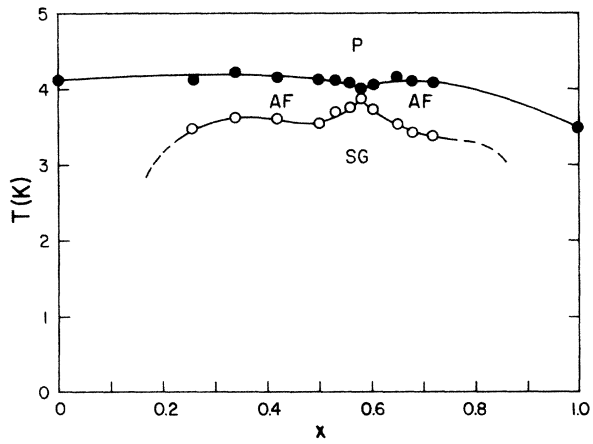

FIG. 6. Phase diagram of temperature vs x (mole fraction of nickel) showing the paramagnetic, antiferromagnetic, and spin-glass regions.

dependence behavior may be due to random fields. Fishman and Aharony[22] showed, for example, that random fields are generated by uniform fields in dilute Ising antiferromagnets. The random-field problem[23,24] and spin-glass theory[25] are similar in that the irreversability and time dependence can be associated with large free-energy barriors whose minima can disappear as the temperature and field are varied. In the random-field case the free-energy minima are associated with domain-wall pinning at impurities. While random-field systems are generally dilute antiferromagnets, undiluted mixed magnetic systems have also been described in terms of random fields. One such example is $Fe_{1-x}Co_xCl_2$ as reported by Wong and Cable.[26] In this system time dependence is seen when the sample is field cooled, but not when zero-field cooled with a magnetic field subsequently applied. This is interpreted as a domain state forming in the field-cooled process, whereas in the zero-field process long-range ordering is obtained.[23] In the CoNiTAC no time dependence is seen upon field cooling, but rather the time-dependent behavior results from magnetic field changes and also causes a cusp in the ac susceptibility versus temperature at zero field.[21] The results on CoNiTAC are therefore discussed in terms of a spin-glass (SG) system.

Both CoTAC and NiTAC, as described in the Introduction, have similar magnetic properties at low temperatures. That is, both are canted antiferromagnets with a net ferromagnetic moment along the a crystallographic axis. The interactions which form the canted three-dimensional spin structures may be quite different and thus introduce the necessary frustration for spin-glass behavior. CoTAC has a very weak antiferromagnetic coupling between ferromagnetically coupled planes. However, the spins are canted because of large single-ion anisotropy. We suggest that a very weak ferromagnetic coupling exists between the planes for NiTAC but, as before, the large single-ion anisotropy forces the canting of the spins and results in the antiferromagnetic behavior in the c direction. The competition between the interplanar ferro- and antiferromagnetic "canting" could then lead to the observed spin-glass behavior. Such a change in sign for weak interplanar coupling accompanied by minor structural change has been observed by us in the diammonium tetrachloro- and tetrabromocuprate systems.[27] Our suggestion that the ferromagnetic coupling is weak in NiTAC is prompted by the single-crystal data which indicate a lower temperature for c-axis antiferromagnetic ordering above 60% Ni and a lower temperature for a-axis ferromagnetic ordering below 60% Ni in the crystals.

The uncertainties shown in Fig. 6 are approximately the size of the data circles so that the existence of a tetracritical point (TCP) and the shape of the tetracritical region cannot yet be confirmed to exist on this phase diagram. The region in our diagram where the TCP might occur is not well defined but appears to be around 60% Ni ($x=0.6$).

The spin-glass region is unusually broad, extending from low to high nickel concentrations. We feel this owes to the pseudo-one-dimensional nature of the crystals. That is, a smaller amount of nickel or cobalt in an otherwise pure sample is necessary to introduce sufficient frustration along the chains to cause entrance into a spin glass as opposed to a strictly three-dimensional magnetic system. This type of very broad spin-glass region was also observed by DeFotis and Mantus[28] in $Co_{(1-x)}Mn_xCl_2\cdot 2H_2O$ which is also a pseudo-one-dimensional system although with considerably higher interchain coupling.

Typically, TRM measurements for spin glasses have been fit to ln$t$ or stretched exponential forms.[29] Neither type of fit was found quite sufficient for the CoNiTAC system. However, by adding a constant M' to the stretched exponential form, times from 10 to 300 sec fit quite well. M' represents the zero-field magnetization expected in a ferromagnetic system such as CoNiTAC along its a axis. Using the functional form of Chamberlin, Mozurkewick, and Orbach[30] with this additional constant we write

$$M_{\mathrm{TRM}}=M_0\exp[-(t/\tau)^{1-n}]+M' . \quad (1)$$

M_0 is set so that $M_{\mathrm{TRM}}(t=0)$ is the initial magnetization before the field is switched off. At a field of 50 Oe in the powder samples, this is in effect the magnetization along the ferromagnetic or a axis since the b and c axes have very small magnetizations under these conditions. The system is in the antiferromagnetic region along the c axis and at all times the magnetization along the b axis is very small. Single-crystal samples were used to determine that only the ferromagnetic or a axis shows TRM behavior, but in order to fit the data the much larger signals from powder samples were used. The three parameters τ, n, and M' were then determined such that the mean-square deviation of the model and the experimental data was minimized. Table II lists these parameters for the temperatures and nickel percentages investigated.

The pseudo-one-dimensional characterization of this compound refers to the fact that there is a strong intrachain exchange with much smaller interchain exchange, the weaker exchange allowing the system to order in

TABLE II. Best fits of the parameters τ, n, and M' to Eq. (1) for TRM measurements at the given temperatures and nickel concentrations.

% Ni	T	τ	n	M'
34	2.4	38.8	0.644	265
34	2.6	12.7	0.610	214
34	2.8	4.43	0.657	161
34	3.0	2.80	0.607	135
34	3.2	1.91	0.589	105
58	2.4	13.2	0.524	324
58	2.6	5.57	0.639	262
58	2.8	2.42	0.670	221
58	3.0	2.94	0.563	189
58	3.2	2.60	0.445	149
72	2.4	22.5	0.427	127
72	2.6	5.32	0.514	69
72	2.8	2.51	0.493	41

three dimensions. It is interesting to ask whether a particular dimensionality can associate the SG behavior in this compound. Grassberger and Proaccia[31] find that a dimensionality of the diffusive space is related to n of Eq. (1) by $n=(1-d)/(d+2)$. Since our values of n vary from 0.4 to 0.67, the corresponding dimensionality d varies from 3 to 1, respectively. CoNiTAC, as we have already considered, seems to derive its frustration from the weak 3D ordering. MnCoTAC and MnNiTAC should be expected to derive a frustration from their 1D ferromagnetic-antiferromagnetic competition. That no spin-glass behavior is observed in these systems is consistent with a critical dimensionality greater than one for the development of spin-glass behavior.

Also, from Table II it is clear that there is a temperature dependence to the relaxation time. Therefore in an attempt to classify the spin-glass region as a function of x, we have made a rough fit to the model of relaxation proposed by Hoogerbeets, Lou, and Orbach[32] for Ag:Mn. Their model is consistent with an exponential distribution if independent, random free-energy levels are assumed to exist in the spin-glass phase; in which case the expression for relaxation is written

$$1/\tau = A \exp[-\alpha(T_g/T)] . \quad (2)$$

A plot of $\ln(1/\tau)$ versus T_g/T from Tables I and II does not show a straight line so that A and α are not constant over our range of temperature, nevertheless there is a definite tendency for faster relaxation as temperature increases. Our very rough values from these plots yield a value for $\alpha=9$ over the entire range of x and values of $A=2\times10^4$ sec^{-1} near the edges ($x=0.26$ and 0.72) and 1×10^5 sec^{-1} for $x=0.58$. These numbers indicate a fast relaxation process compared to $\alpha=2.5$ and $A=10^{-3}$ sec^{-1} for Ag:Mn. We find that the temperature dependence of M' follows the behavior of T; that is, it is largest at low temperatures, almost disappearing near T_g. Further, for a given temperature in the SG region, our numbers show a tendency for the overall relaxation processes to be faster near the "edges" of the SG region where the systems behave more like the unmixed compounds and slower in the center where the mixture is more complete.

CONCLUSIONS

The pseudo-one-dimensional mixed system, CoNiTAC has been found to exhibit spin-glass behavior below a temperature, T_g, while the MnCoTAC and MnNiTAC systems do not. The phase diagram of temperature versus x shows a very broad and deep spin-glass region with unusually thin antiferromagnetic phase regions above it. Evidence for a tetracritical point near $x=0.6$ is indicated. Thermoremanent magnetization versus time below T_g has been fit to a stretched exponential function plus a constant offset.

ACKNOWLEDGMENTS

We thank Professor Gary C. DeFotis for helpful discussions and a reading of the manuscript. This work was supported by National Science Foundation Grant Nos. DMR-8403993 and DMR-8702933.

[1]See P. W. Anderson, in *Ill-Condensed Matter*, edited by R. Balian, R. Maynard, and G. Toulouse (North-Holland, Amsterdam, 1980), and references therein.
[2]H. K. Fisher, Phys. Status Solidi B **116**, 357 (1983).
[3]J. A. Mydosh, in *Lecture Notes in Physics*, edited by C. Castelloni *et al.* (Springer, Berlin, 1981).
[4]H. K. Fisher, Phys. Status Solidi B **130**, 13 (1985).
[5]K. Binder and A. P. Young, Rev. Mod. Phys. **58**, 801 (1986).
[6]D. B. Lossee, J. N. McElearny, G. E. Shankle, and R. L. Carlin, Phys. Rev. B **8**, 2185 (1973).
[7]R. D. Spence and A. C. Botterman, Phys. Rev. B **9**, 2993 (1974).
[8]H. A. Groenendijk and A. J. van Duyneveldt, Physica **B115**, 41 (1982).
[9]A. J. van Duyneveldt, J. Appl. Phys. **53**, 8006 (1982).
[10]S. O'Brien, R. M. Gavra, C. P. Landee, and R. D. Willett, Solid State Commun. **39**, 1333 (1981).
[11]R. Hoogerbeets, S. A. J. Wiegers, A. J. van Duyneveldt, R. D. Willett, and V. Geiser, Physica **B125**, 135 (1984).
[12]R. Hoogerbeets, A. J. van Duyneveldt, and C. H. W. Swuste, Physica **B128**, 218 (1985).
[13]R. E. Caputo, R. D. Willett, and J. A. Muir, Acta Crystallogr. Sect. B **32**, 2639 (1976).
[14]W. Depmeier and K. H. Klaska, Acta Crystallogr. Sect. B **36**, 1065 (1980).
[15]S. Simizu, J. Y. Chen, and S. A. Friedberg, J. Appl. Phys. **55**, 2398 (1984).
[16]R. Megy, E. Velu, and J. P. Renard, J. Magn. Magn. Mater. **54**, 1271 (1986).
[17]J. C. Schouten, K. Takeda, and K. Kopinga, J. Phys. (Paris)

Colloq. **39**, C6-723 (1978).
[18]I. Matsubara, K. Iio, and K. Nagata, J. Chem. Soc. Jpn. **51**, 3071 (1982).
[19]A. C. Phaff, C. H. W. Swuste, and W. J. M. de Jonge, Phys. Rev. B **25**, 6570 (1982).
[20]M. J. Lindbeck, Ph.D. thesis, Montana State University, 1983.
[21]G. V. Rubenacker, D. N. Haines, and J. E. Drumheller (unpublished).
[22]S. Fishman and A. Aharony, J. Phys. C **12**, L729 (1979).
[23]H. Yoshizawa and D. P. Belanger, Phys. Rev. B **30**, 5220 (1984).
[24]C. Ro, G. S. Grest, C. M. Soukoulis, and K. Levin, Phys. Rev. B **31**, 1682 (1985).
[25]C. M. Skoukoulis, K. Levin, and G. S. Grest, Phys. Rev. B **28**, 1495 (1983).
[26]P. Wong and J. W. Cable, Solid State Commun. **51**, 545 (1984).
[27]G. V. Rubenacker, D. N. Haines, J. E. Drumheller, and K. Emerson, J. Magn. Magn. Mater. **43**, 238 (1984).
[28]G. C. DeFotis and D. S. Manus, J. Magn. Magn. Mater. **54**, 79 (1986); (private communication).
[29]R. G. Palmer, D. L. Stein, E. Abrahams, and P. W. Anderson, Phys. Rev. Lett. **53**, 958 (1984).
[30]R. V. Chamberlain, G. Mosurkewich, and R. Orbach, Phys. Rev. Lett. **52**, 867 (1984).
[31]P. Grassberger and I. Procaccia, J. Chem. Phys. **77**, 6281 (1982).
[32]R. Hoogerbeets, Wei-Li Luo, and R. Orbach, Phys. Rev. Lett. **55**, 111 (1985).